Structure and optical anisotropy of $K_{1.75}(NH_4)_{0.25}SO_4$ solid solution

[1, 2] Shchepanskyi P. A., [1] Kushnir O. S., [1] Stadnyk V. Yo., [3] Fedorchuk A. O., [1, 2] Rudysh M. Ya., [1] Brezvin R. S., [1] Demchenko P. Yu. and [4] Krymus A. S.

[1] Ivan Franko National University of Lviv, 8 Kyrylo and Mefodiy Street, 79005 Lviv, Ukraine, pavloshchepanskyi@gmail.com
[2] J. Dlugosz Academy of Czestochowa, Armii Krajowej 13/15, PL-42-201 Czestochowa, Poland
[3] Lviv National University of Veterinary Medicine and Biotechnologies, 50 Pekarska Street, 79010 Lviv, Ukraine
[4] Eastern European National University, 13 Volya Avenue, 43025 Lutsk, Ukraine

Abstract. In this work we have grown single crystals $K_x(NH_4)_{2-x}SO_4$ ($x \approx 1.75$), which belong to a potassium–ammonium sulfate family, and studied their room–temperature structure. Spectral dependences of the principal refractive indices and principal optical birefringences are measured in the visible region. Anomalous birefringence dispersion is observed along the light propagation direction parallel to the principal x axis. According to our birefringence extrapolation based on the Sellmeier fit for the refractive indices, the symmetry of optical indicatrix at the room temperature should increase at the light wavelength $\lambda_{IP} \approx 1350 \pm 60$ nm. This corresponds to a specific 'isotropic point' defined by the condition $n_x(\lambda_{IP}) = n_y(\lambda_{IP})$, which has not been detected in either K_2SO_4 or $(NH_4)_2SO_4$ crystals.

1. Introduction

Inversion of sign of the optical birefringence (an iso-index, zero-crossing birefringence or, simply, 'isotropic' point abbreviated hereafter as IP) represents a result of accidental increase in the symmetry of optical indicatrix, which is not governed by the Neumann's principle. It is observed as disappearance of linear optical birefringence in an (otherwise anisotropic) crystal, which happens at some wavelength, temperature and pressure. The effect, which has been found in CdSe [1], CdS [2–4], ZnO [3], $AgGaS_2$ [5] and many other crystals, has attracted much attention of researchers. From the fundamental point of view, there are many interesting phenomena occurring near the IP or immediately at this point (see, e.g., Refs. [3, 4, 6–10]). It is enough to remind that the effects of energy transfer between the normal light waves in the vicinity of IP have stimulated elaboration of a canonical coupled-mode theory [11]. On the other hand, the IP-related effects have found numerous applications ranging from temperature or pressure measuring to constructing narrow-band optical filters and determining the exact content of a substance [11–15].

There are two points that stimulate searches for new crystalline materials with the IP. The first is that many materials found up to now are inherently imperfect due to specific melt-based growing techniques. Then the very spectral position of the IP and the corresponding material para-

meters depend notably on the growing conditions, stoichiometry and the impurities involved and, therefore, vary from sample to sample. For instance, even such basic parameter as the wave-coupling coefficient in wurtzites is heavily determined by the internal mechanical stresses in crystal samples [3, 4, 8, 16]. To overcome this deficiency, it would be desirable to work with solution-grown crystals revealing more stable and reproducible characteristics. Besides, the characteristics associated with the IP can become instable with respect to temperature or pressure, whenever the material manifests structural transformations. The second point is that the IP is often not located in a desirable spectral region or appears at temperatures different from ambient one, which requires technically complex stabilization facilities. In this respect, isomorphic substitutions can efficiently change the spectral and temperature positions of the IP. This is a reason why mixed crystals with varying content or solid solutions with the IP have been studied so extensively (see, e.g., Refs. [9, 12, 15, 17–20]). On the other hand, efficient control of the IP characteristics anticipates also ascertaining the underlying interrelations between the structural and optical anisotropy characteristics.

The arguments mentioned above have drawn our attention to K_2SO_4–$(NH_4)_2SO_4$ crystals of a potassium–ammonium sulfate (PAS) system, which is known to form a continuous series of isomorphic solid solutions with a general formula $K_x(NH_4)_{2-x}SO_4$ ($0 < x < 2$). They are described by the point symmetry group *mmm* at the room temperature. The structure and various physical properties of pure K_2SO_4 and $(NH_4)_2SO_4$ have been studied in a number of works (see, e.g., Refs. [21–23]). In particular, the IP has not been found in ammonium sulfate, while potassium sulfate reveals a peculiar isotropic state at relatively high temperatures (500–600 K), which hinders any practical applications. The properties of the PAS solid solutions have also been investigated, though mainly in connexion with their thermal structural transformations [24–26]. To our knowledge, no optical studies of PAS with intermediate fractions $0 < x < 2$ have been undertaken up to date. However, it is known that increasing x value suppresses the paraelectric-to-ferrielectric phase transition occurring at 223 K in pure $(NH_4)_2SO_4$. What is important, this phase transition in the PAS system disappears completely at $x > 1.4$ [24] and the crystals become thermally stable, since the hexagonal-to-orthorhombic phase transition occurring in K_2SO_4 at very high temperatures (~ 860 K) cannot affect the room-temperature properties of PAS.

Below we report the structure and spectral dependences of the refractive indices and the optical birefringence in a particular PAS representative, $K_{1.75}(NH_4)_{0.25}SO_4$. The main subject is the optical anisotropy in relation to the structural features of the crystal, and searching for the IP.

2. Experimental

Single crystals of mixed PAS were grown from aqueous solution, using the version of a standard slow-evaporation technique reported in Refs. [24, 26]. Commercially available salts K_2SO_4 and $(NH_4)_2SO_4$ with the purity not lower than 99.9% served as initial components. All the crystals grown in this manner had a shape of elongated prisms, with the size ~ 1 cm^3. They were optically transparent and revealed a perfect visual quality under polarization microscope.

For X-ray diffraction studies, single crystalline samples were carefully pulverized in agate mortar and a resulting powder was deposited onto polymeric film in a uniform layer, put in a cuvette and fixed with a covering film. The sets of experimental diffraction intensities and reflection angles 2θ from the samples under examination were obtained, using an automatic STOE STADI P diffractometer with a linear position-sensitive detector. The apparatus worked in a transmission mode according to a modified Guinier geometry. The main parameters were as follows: Cu-$K\alpha_1$ radiation, the electric voltage $U = 40$ kV and the current $I = 37$ mA, a concave

Ge-monochromator (111) of a Johann type, and a $2\theta/\omega$-scanning. The temperature of the measurements was kept at $T = 23.0\pm0.5°C$. Initial processing of the experimental diffraction data, calculation of theoretical diffractions and indexing of the unit-cell parameters were performed using a STOE WinXPOW software package [27] and a PowderCell [28] method. The latter compared the X-ray diffraction profiles obtained experimentally with both theoretical and experimental diffraction patterns available for the system under test.

We measured refractive indices n_i of the PAS solid solution for the principal axes $i = x, y$ and z of optical Fresnel ellipsoid ($x = a$, $y = b$ and $z = c$), using a standard immersion method. A mixture of α-monobromnaftalyn and refined petroleum was employed as an immersion liquid. The experimental apparatus included a detachable Obreimov device and an IRF-23 refractometer equipped with a temperature-control system ($T = 23.0\pm0.1°C$). When studying dependences $n_i(\lambda)$ on the light wavelength λ, we used a monochromator ZMR-3 and a xenon lamp DKSSh-1000 as a light source, which demonstrated a high light yield and low noises in our working wavelength region (450–720 nm). The polarization of light was controlled using commercial Glan prisms. The resulting measurement accuracy δn was not worse than $\pm2\times10^{-4}$.

Optical birefringences Δn_i of PAS along the principal axes were studied with a standard spectral photometric method, which was based upon measuring optical transmittance of a polarizer–sample–analyzer, with the sample orientated diagonally in between crossed polarizers. The reference birefringence values were determined issuing from the n_i data. The spectral dependences $\Delta n_i(\lambda)$ were obtained at the same temperature and in the same wavelength region as in the refractive-index studies. We used a DFS-8 spectrograph with the dispersion 0.5 nm×mm^{-1} and the resulting resolution about 0.5–1.0 nm. The total birefringence error amounted to $\delta\Delta n = \pm2\times10^{-5}$.

3. Results and their discussion
3.1. Crystal structure
An example of experimental difractograms obtained for our PAS powder is presented in Fig. 1. We have taken the results of structural studies [26] as an initial model and so adopted the space group *Pnma* (No 62) for the compound under test. Then the structure of our PAS crystals has been refined using a Rietveld method and a WinCSD program complex [29]. The structural parameters have been specified assuming that the texture axis is parallel to the direction [2 1 2] and the structural factor is equal to 0.31(2), with the corresponding difference factors being equal to $R_I = 0.0887$ and $R_P = 0.2142$. The refined results for the PAS structure are displayed in Table 1.

The chemical composition of our PAS crystals has been determined following from the unit-cell parameters found experimentally and the 'concentration dependences' $a(x)$, $b(x)$ and $c(x)$ reported in Ref. [24]. The corresponding results have been finalized with the Rietveld method, using the occupation numbers for G-positions of the potassium and nitrogen atoms. According to our data, we deal with the compound $K_{1.75}(NH_4)_{0.25}SO_4$. Although the above technique does not rely directly on the data of chemical analysis, it provides quite sufficient accuracy for the substitution parameter (x ≈ 1.75±0.02).

The crystalline structure of our PAS compound can be considered as an assembly of $[SO_4]^{2-}$ tetrahedrons located in the positions of anionic sublattice, where cation atoms are located in the cavities among the anions (see Fig. 2). To get further insight into the structural features of PAS, we have employed a second-anion coordination approach (see Ref. [30]). The second-anion coordination of the anion atoms corresponds to a hexagonal analogue of cuboctahedron.
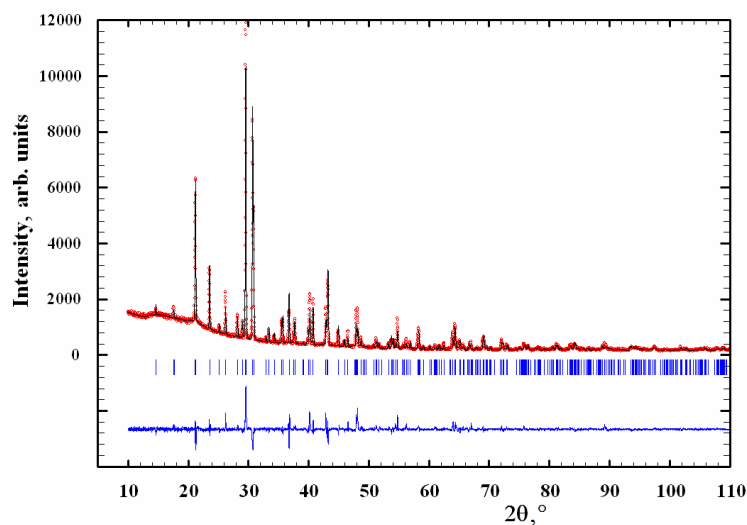
Fig. 1. Experimental (open red circles), theoretical (upper black solid line) and differential (lower blue solid line) diffractograms obtained for our PAS crystals, along with Bragg-reflection marks (blue vertical bars) determined for their refined structure.

Table 1. Wyckoff positions, fractional atomic coordinates x/a, y/b and z/c, and isotropic thermal displacement factor B obtained for our PAS crystals. The lattice parameters are equal to $a = 7.5562(3)$, $b = 5.7917(2)$ and $c = 10.1016(4)$ Å, and the cell volume is $442.08(5)$ Å^3. The figures in parentheses represent standard deviations.

Atom	Wyckoff position	x/a	y/b	z/c	B, Å^2
S1	$4c$	0.2352(5)	1/4	0.0784(6)	0.60(13)
O1	$8d$	0.3001(9)	0.0405(8)	0.1445(7)	0.40(2)
O2	$4c$	0.0500(2)	1/4	0.0890(1)	1.80(4)
O3	$4c$	0.7900(2)	1/4	0.5567(9)	1.10(4)
M* = 0.75[K] + 0.25[NH$_4$]	$4c$	0.1800(5)	1/4	0.4087(5)	1.14(14)
K	$4c$	0.4869(5)	1/4	0.7029(4)	1.13(11)
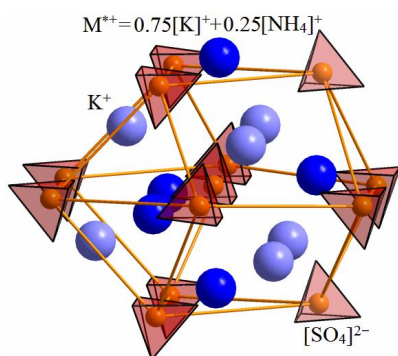
Fig. 2. Second-anion coordination of structural components in the K$_{1.75}$(NH$_4$)$_{0.25}$SO$_4$ solid solution crystals. Dark blue spheres M*$^+$ denote 'statistical-mixture cations' (see text).

As seen from Fig. 2 and Fig. 3, the potassium atoms, which are not substituted with the ammonium groups, occupy octahedral positions, whereas 'statistical-mixture atoms' represented conventionally as M* = 0.75[K] + 0.25[NH$_4$] are arranged inside twin tetrahedral cavities. We suppose that the main feature of the structure of our PAS compound, the 'statistical mixture' M*
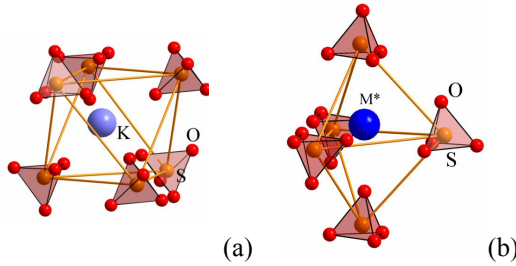
Fig. 3. Coordination of potassium atoms (a) and 'statistical-mixture atoms' $M^* = 0.75[K] + 0.25[NH_4]$ (b) in the structure of $K_{1.75}(NH_4)_{0.25}SO_4$.

mentioned above, can notably affect different physical properties of the crystal and, in particular, its optical characteristics. This is caused by asymmetric arrangement of the anion atoms inside trigonal dipyramids. In fact, increasing fraction of ammonium ($M^* \neq K$) leads to some asymmetry in the local structure accompanied by changes in the nearest-neighbour coordination environment and deformations of overlapping orbitals, thus inducing changes in the physical properties.

3.2. Refractive indices and optical anisotropy

The band structure, dielectric function and the corresponding optical absorption spectra in a wide spectral range will be reported elsewhere [31]. Here we notice only that our theoretical calculations of the bandgap E_g for $K_{1.75}(NH_4)_{0.25}SO_4$ performed in the local-density and generalized-gradient approximations for the density functional have yielded in $E_g \approx 4.9$ eV. The theoretical dandgap appears to be somewhat lower than the experimental value ~ 6.8 eV, as expected for the above approximations. The latter E_g value is larger than the corresponding parameter for $(NH_4)_2SO_4$ (4.5 eV) and smaller than that known for K_2SO_4 (7.2 eV). In line with a relatively small fraction x, the parameters E_g for our PAS solid solution and K_2SO_4 are essentially closer. The relevant fundamental absorption edge for PAS is about 180 nm. Finally, the long-wavelength absorption is located in the far-infrared range, thus confirming that the infrared effective oscillators affect the spectral dependences of refractive indices in the visible region much less than their ultraviolet counterparts (see discussion below).

The spectral dependences of the refractive indices measured for $K_{1.75}(NH_4)_{0.25}SO_4$ at the room temperature are presented in Fig. 3. Quite expectedly, the refractive dispersion is normal for all light-wave polarizations. The refractive index for the polarization along the *y* axis, which is normal to the plane *xz* of optic axes, acquires a middle value, whereas the index for the *z* polarization parallel to the acute bisector of the optic axes is the smallest, i.e. we have $n_z > n_y > n_x$. These inequalities imply that the PAS crystals are optically positive. Moreover, as seen from Fig. 4, the spectral changes in the refractive indices satisfy the relation $|dn_y/d\lambda| > |dn_{x,z}/d\lambda|$.
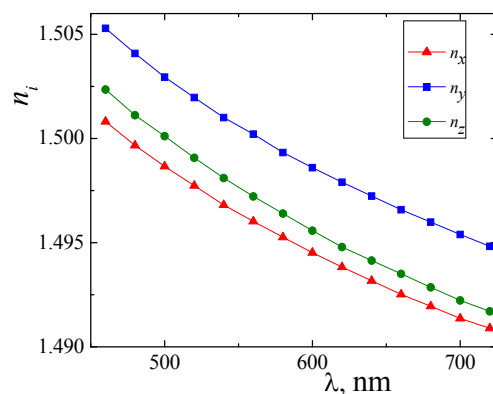
Fig. 4. Refractive index dispersions measured for the $K_{1.75}(NH_4)_{0.25}SO_4$ crystals at the room temperature: n_x (green circles), n_y (blue squares) and n_z (red triangles).

The behaviour of the refractive indices can be interpreted using a known Lorentz–Lorenz formula:

$$\frac{n_i^2 - 1}{n_i^2 + 2} = \frac{4}{3}\pi N_0 \alpha_i = \frac{\rho}{\mu} R_i ,\tag{1}$$

where ρ is the density of crystal, μ its molar mass, N_0 the Avogadro number, and α_i and R_i denote respectively electronic polarizabilities and molar refractivities for the light waves polarized along different principal axes i. A closer insight into refractive dispersion in the visible region can be got using a two-oscillator Sellmeier formula,

$$n_i^2(\lambda) = 1 + \frac{B_i \lambda_{U,i}^2 \lambda^2}{\lambda_{U,i}^2 - \lambda^2} + \frac{B'_i \lambda_{I,i}^2 \lambda^2}{\lambda_{I,i}^2 - \lambda^2} \approx 1 + \frac{B_i \lambda_{U,i}^2 \lambda^2}{\lambda_{U,i}^2 - \lambda^2} - B'_i \lambda^2 .\tag{2}$$

Here the parameters B_i and B'_i are associated with the strength, the effective mass and the charge of ultraviolet and infrared oscillators, respectively, while $\lambda_{U,i}$ and $\lambda_{I,i}$ denote the effective positions of the corresponding ultraviolet (the subscript U) and infrared (the subscript I) absorption bands. Since $\lambda_{I,i}$ are of the order of 10–20 μm, one can simplify the contribution of infrared oscillator into the $n_i(\lambda)$ functions to the last term appearing in the r. h. s. of Eq. (2). The experimental values of the parameters entering Eqs. (1) and (2) are presented in Table 2.

Table 2. Refractive parameters derived for the $K_{1.75}(NH_4)_{0.25}SO_4$ crystals at the room temperature.

Principal axis	$\lambda_{U,i}$, nm	B_i, 10^{-6} nm^{-2}	B'_i, 10^{-9} nm^{-2}	α_i, 10^{-24} cm^3 (at $\lambda = 500$ nm)	R_i, cm^3 (at $\lambda = 500$ nm)
x	76.09	211.5	30.09	7.737	19.52
y	80.09	191.0	29.85	7.756	19.56
z	78.97	198.0	29.14	7.795	19.66

When compared with the relevant data for the pure K_2SO_4 crystals [21], the spectral dependences of refractive indices are similar for the x and y directions, while the refractive index for the z polarization in $K_{1.75}(NH_4)_{0.25}SO_4$ is slightly higher. The upward shift in the refractive index values observed for PAS is equal to 1.2×10^{-3}. If compared with pure K_2SO_4, the refractive parameters of our PAS crystals are also somewhat different. In particular, the Sellmeier parameters B_i are larger by about 50×10^{-6} nm^{-2} and $\lambda_{U,I}$ are shifted towards the short-wavelength side by ~ 12 nm. The polarizabilities α_i and the molar refractivities R_i of PAS are slightly larger than those of K_2SO_4.

Our studies of optical birefringence Δn_i at the room temperature (see Fig. 5) have shown that the dispersion $\Delta n_i(\lambda)$ for the propagation directions y and z is normal, with the rough averages being equal to $d\Delta n_y/d\lambda \approx -1.0 \times 10^{-6}$ nm^{-1} and $d\Delta n_z/d\lambda \approx -1.6 \times 10^{-6}$ nm^{-1}. On the contrary, the birefringence dispersion $\Delta n_x(\lambda)$ has anomalous character ($d\Delta n_x/d\lambda \approx 0.9 \times 10^{-6}$ nm^{-1}). These facts hint that an IP can exist in the PAS crystals somewhere in the near-infrared spectral region.

A simple comparison of our birefringence data obtained for the PAS crystals with the results found earlier for K_2SO_4 [21] reveals the following facts. On average, the Δn values for the propagation directions y and z for potassium sulphate are slightly higher ($d\Delta n_y/d\lambda \approx -2.6 \times 10^{-6}$ nm^{-1}) and lower ($d\Delta n_z/d\lambda \approx 3.6 \times 10^{-7}$ nm^{-1}), respectively. The most significant difference is observed for the birefringence measured along the x axis. The latter remains normal for K_2SO_4 ($d\Delta n_x/d\lambda \approx -1.9 \times 10^{-6}$ nm^{-1}) but becomes anomalous ($d\Delta n_x/d\lambda \approx 0.9 \cdot 10^{-6}$ nm^{-1}) for $K_{1.75}(NH_4)_{0.25}SO_4$.
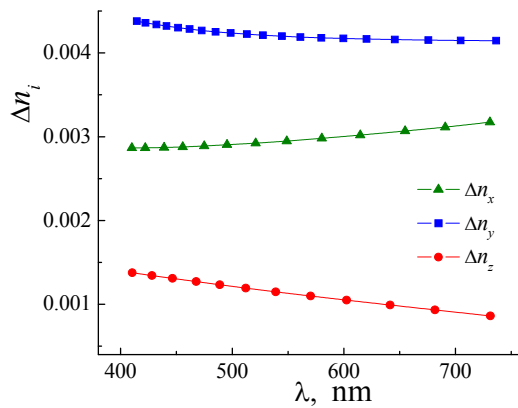
Fig. 5. Optical birefringence dispersions measured for the $K_{1.75}(NH_4)_{0.25}SO_4$ crystals at the room temperature: Δn_x (green triangles), $-\Delta n_y$ (blue squares) and Δn_z (red circles).

Now we discuss in a more detail the availability of IP in our PAS crystals. Let us use a standard summation rule $\sum_i \Delta n_i = 0$ ($i = x,\ y,\ z$) for the optical birefringences referred to different propagation directions, where the definitions involve circular permutations: e. g., $\Delta n_x = n_z - n_y$, $\Delta n_y = n_x - n_z$ and $\Delta n_z = n_y - n_x$. Since the relations $n_z > n_y > n_x$ hold true for $K_{1.75}(NH_4)_{0.25}SO_4$, the birefringences along the x and z axes are positive and that along the y axis is negative. Of course, it is hardly believable that all of the refractive indices can accidentally become equal to each other ($n_x = n_z = n_y$) at some wavelength. However, there still remains a more specific possibility, a case of equality of only two of the indices. Then a possible IP λ_{IP} in a more practical near-infrared region is defined by the relations $\Delta n_z(\lambda_{IP}) = 0$ or $-\Delta n_y(\lambda_{IP}) = \Delta n_x(\lambda_{IP})$, which are quite equivalent theoretically but independent from the viewpoint of experimental data. Unfortunately, there is a lack of direct, firmly grounded phenomenological relationships for the birefringence dispersion. Therefore we start from the Sellmeier formulae (2) for the refractive indices and express the birefringences $\Delta n_i = n_j - n_k$ in terms of n_j and n_k. Then the parameters of Eq. (2) are recalculated basing on the much more accurate experimental birefringence data. Issuing from the latter parameters, one can fit the $\Delta n_i(\lambda)$ data, extrapolate the theoretical curves into the near-infrared region and find the spectral position λ_{IP} in our PAS crystals (see Fig. 6). The λ_{IP} parameter searched for is equal to $\lambda_{IP} \approx 1350\pm60$ nm. Here the accuracy has been estimated after varying, in the limits of standard deviations, the most critical terms in Eq. (2) that involve the effective $\lambda_{U,i}$ wavelengths. Note that the equality $n_x(\lambda_{IP}) = n_y(\lambda_{IP})$ has also been confirmed by fitting directly $n_x(\lambda)$ and $n_y(\lambda)$ data, though with essentially lower accuracy ($\lambda_{IP} \sim 1400\pm200$ nm).
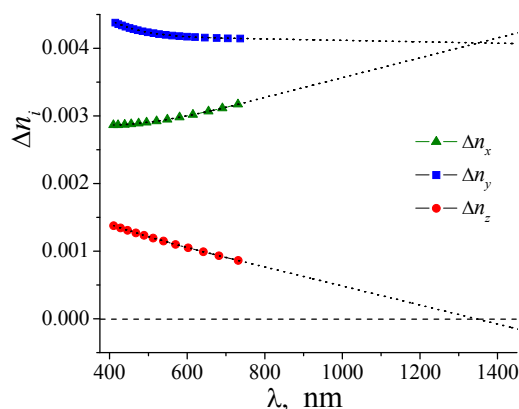
Fig. 6. Long-wavelength extrapolations of optical-birefringence dispersion curves for the $K_{1.75}(NH_4)_{0.25}SO_4$ crystals, as made basing on the Sellmeier formulae for the refractive indices (see text): Δn_x (green triangles), $-\Delta n_y$ (blue squares) and Δn_z (red circles).

Hence, although the optical indicatrix in the biaxial PAS crystals has the shape of a general ellipsoid ($n_z \neq n_y \neq n_x$), it becomes an ellipsoid of revolution ($n_y = n_x \neq n_z$) at the IP. Of course, this IP is rather specific: no optically isotropic state is observed for arbitrary wave-normal directions, as is the case with the IP occurring in optically uniaxial crystals. The PAS crystal becomes free of linear refractive anisotropy only for a single propagation direction z, which represents analogue of the optic axis in uniaxial crystals. Nevertheless, this kind of IP does correspond to its general definition as a state in which the optical indicatrix manifests an accidental, 'local' symmetry increase, if compared with the predictions of Neumann's principle.

It is clearly seen from our simulations that the IP represents a delicate result of competition among the contributions of short- and long-wavelength oscillators to the refractive indices. In this respect it is worth reminding that the both limiting compounds with x = 0 and x = 2 in the PAS system reveal no IPs at the room temperature, so that the latter appears only due to a moderate (12.5%) isomorphic substitution of K with NH_4. In this sense the PAS system is similar to $LiNb_{1-x}Ta_xO_3$ where a small addition of lithium niobate to the tantalate also produces the IP at the room temperature [17]. Finally, thermal stability and absence of phase transitions in a wide region including the room temperature can make the $K_{1.75}(NH_4)_{0.25}SO_4$ crystals a good candidate for different applications in the fields of crystal optical sensing and operation of laser light. The other suitable circumstance is that the IP at $\lambda_{IP} \approx 1350$ nm falls into the spectral region where standard semiconductor LEDs operate.

4. Conclusions

In the present work we report the structure and basic optical properties of a PAS solid solution, which has been grown using the slow-evaporation technique. Basing on the experimental X-ray diffraction data, we have revealed the structural characteristics of our single crystals under ambient conditions and determined their content to be $K_{1.75}(NH_4)_{0.25}SO_4$ (x $\approx$ 1.75$\pm$0.02). The crystal structure has been refined using the second-anion coordination approach. It is found that potassium occupying octahedral positions is not substituted with the ammonium group, whereas the potassium atoms located inside twin tetrahedral cavities are partly substituted, forming a 'statistical mixture' M* = 0.75[K] + 0.25[NH_4]. It is supposed that this feature can impose specific physical properties of the crystal due to asymmetry of trigonal dipyramids of the anions.

The basic optical properties of $K_x(NH_4)_{2-x}SO_4$ are ascertained at the room temperature in the visible spectral region. To our knowledge, this is the first optical study of the PAS-family crystals at the intermediate (0 < x < 2) potassium fraction x. In compliance with a moderate (12.5%) degree of isomorphic K $\rightarrow$ NH_4 substitution, the fundamental absorption edge, the refractive indices and the birefringences are in general closer to those of pure potassium sulfate than its ammonium counterpart. The $K_{1.75}(NH_4)_{0.25}SO_4$ single crystals are optically positive and manifest a normal refractive dispersion. The substitution K $\rightarrow$ NH_4 increases all of the refractive indices and the refractive dispersion for the light polarized along the y direction. As for the quantitative refractive parameters, we observe a shift in the spectral positions of the effective ultraviolet oscillators towards shorter wavelengths and increase in the strengths of these oscillators.

The dispersion of optical birefringence in PAS is normal for the light propagation directions parallel to the principal axes y and z and anomalous for the x axis. This leads to increasing symmetry of optical indicatrix at the wavelength $\lambda_{IP} \approx 1350\pm60$ nm and the room temperature, which corresponds to the equalities $n_x = n_y$ or $\Delta n_z = 0$. This phenomenon has earlier been observed for neither of the limiting compounds in the PAS system, K_2SO_4 and $(NH_4)_2SO_4$. In other words,

small isomorphic substitutions of potassium with ammonium move the IP from the high-temperature region ($\sim$ 500–600 K) towards the room temperature. As a consequence, $K_{1.75}(NH_4)_{0.25}SO_4$ can be considered as a promising material for IP-based applications in the near-infrared region, where commercial LEDs operate. The optical phenomena occurring in the vicinity of this specific IP will be a subject of our forthcoming study.

References

1. Wardzynski W, 1961. Dichroism and birefringence of single crystals of cadmium selenide. Proc. Roy. Soc. A. **260**: 370–378.

2. Bieniewski T M and Czyzak S J, 1963. Refractive indexes of single hexagonal ZnS and CdS crystals. J. Opt. Soc. Amer. **53**: 496–497.

3. Hopfield J J and Thomas D G, 1965. Polariton absorption lines. Phys. Rev. Lett. **15**: 22–24.

4. Henry C H, 1966. Coupling of electromagnetic waves in CdS. Phys. Rev. **143**: 627–633.

5. Hobden M V, 1967. Optical activity in a non-enantiomorphous crystal silver gallium sulphide. Nature. **216**: 678.

6. May M, Debrus S, Amzallag J and Hui X-M, 1992. Natural optical activity and the anisotropic absorbing properties of $CdGa_2S_4$. J. Opt. Soc. Amer. A. **9**: 1412–1418.

7. Kushnir O and Vlokh O, 1995. Propagation of light in birefringent optically active crystals possessing linear dichroism. Proc. SPIE. **2648**: 585–595.

8. Kushnir O S, Dzendzelyuk O S, Hrabovskyy V A and Vlokh O G, 2004. Optical transmittance of dichroic crystals with "isotropic point". Ukr. J. Phys. Opt. **5**: 1–5.

9. Glazer A M, Zhang N, Bartasyte A, Keeble D S, Huband S and Thomas P A, 2010. Observation of unusual temperature-dependent stripes in $LiTaO_3$ and $LiTa_xNb_{1-x}O_3$ crystals with near-zero birefringence. J. Appl. Cryst. **43**: 1305–1313.

10. Glazer A M, Zhang N, Bartasyte A, Keeble D S, Huband S, Thomas P A, Gregora I, Borodavka F, Marguerone S and Hlinka J, 2012. $LiTaO_3$ crystals with near-zero birefringence. J. Appl. Cryst. **45**: 1030–1037.

11. Yariv A and Yeh P. Optical waves in crystals: propagation and control of laser radiation. New York: Wiley (2003).

12. Laurenti J P, Rustagi K C and Rouzeyre M, 1976. Optical filters using coupled light waves in mixed crystals. Appl. Phys. Lett. **28**: 212–213.

13. Romanyuk M O, Andriyevsky B, Kostetsky O, Romanyuk M M and Stadnyk V, 2002. Crystal optical method for temperature measuring. Condens. Matter Phys. **5**: 579–586.

14. Romanyuk M O and Romanyuk M M, 2005. Inversion of the sign of birefringence and its application in thermometry. Ferroelectrics. **317**: 57–61.

15. Bäumer Ch, Berben D, Buse K, Hesse H and Imbrock J, 2003. Determination of the composition of lithium tantalate crystals by zero-birefringence measurements. Appl. Phys. Lett. **82**: 2248–2250.

16. Kushnir O S, Grabovski V A, Dzendzelyuk O S and Lutsiv-Shumski L P, 2000. Light propagation in wurtzite-type crystals with the Jones calculus. Proc. SPIE. **4148**: 123–128.

17. Wood I G, Daniels P, Brown R H and Glazer A M, 2008. Optical birefringence study of the ferroelectric phase transition in lithium niobate tantalate mixed crystals: $LiNb_{1-x}Ta_xO_3$. J. Phys.: Condens. Matter. **20**: 235237.

18. Stadnyk V Yo, Brezvin R S, Rudysh M Ya, Shchepanskyi P A, Gaba V M and Kogut Z A, 2014. On isotropic states in α-$LiNH_4SO_4$ crystals. Opt. Spectrosc. **117**: 756–758.

19. Rudysh M Ya, Brik M G, Khyzhun O Y, Fedorchuk A O, Kityk I V, Shchepanskyi P A, Stadnyk V Yo, Lakshminarayana G, Brezvin R S, Bak Z and Piasecki M, 2017. Ionicity and birefringence of α-LiNH4SO4 crystals: ab initio DFT study, X-ray spectroscopy measurements. RSC Adv. **7**: 6889–6901.

20. Huband S, Keeble D S, Zhang N, Glazer A M, Bartasyte A and Thomas P A, 2017. Crystallographic and optical study of $LiNb_{1-x}Ta_xO_3$. Acta Cryst. B. **73**: 498–506.

21. Stadnyk V Yo, Romanyuk M O, Chyzh O Z and Vachulovych V F, 2007. The baric changes of the refractive properties of K_2SO_4 crystals. Condens. Matter Phys. **10**: 45–50.

22. El-Korashy A, El-Zahed H and Radwan M, 2003. Optical studies of $(NH_4)_2SO_4$ single crystal in the paraelectric phase. J. Phys. Chem. Solids. **64**: 2141–2146.

23. Lloveras P, Stern-Taulats E, Barrio M, Tamarit J-Ll, Crossley S, Li W, Pomjakushin V, Planes A, Mañosa Ll, Mathur N D and Moya X, 2015. Giant barocaloric effects at low pressure in ferrielectric ammonium sulphate. Nature Commun. **6**: 8801.

24. Shaman A M, Ahmed S, Kamel L and Badr Y, 1987. Structural changes of $((NH_4)_{1-x}K_x)_2SO_4$ crystals. Phys. stat. sol. (a). **100**: 115–119.

25. Petrugevskii V M and Sherman W F, 1993. On the non-statistical substitution of potassium with ammonium in the K_2SO_4–$(NH_4)_2SO_4$ system. J. Mol. Struct. **294**: 171–174.

26. González-Silgo C, Solans X, Ruiz-Pérez C, Martínez-Sarrión M L, Mestres L and Bocanegra E, 1997. Study on the mixed crystals $[NH_4]_{2-x}K_xSO_4$. J. Phys.: Condens. Matter. **9**: 2657–2669.

27. STOE & Cie GmbH, WinXPOW 3.03. Powder diffraction software package. Darmstadt, Germany (2010).

28. Kraus W and Nolze G, 1996. POWDER CELL – a program for the representation and manipulation of crystal structures and calculation of the resulting X-ray powder patterns. J. Appl. Cryst. **29**: 301–303.

29. Akselrud L and Grin Y J, 2014. WinCSD: software package for crystallographic calculations (Version 4). Appl. Cryst. **47**: 803–805.

30. Fedorchuk A O, Parasyuk O V and Kityk I V, 2013. Second anion coordination for wurtzite and sphalerite chalcogenide derivatives as a tool for the description of anion sub-lattice. Mater. Chem. Phys. **139**: 92–99.

31. Shchepanskyi P A, Gaba V M, Stadnyk V Yo, Rudysh M Ya, Piasecki M and Brezvin R S, 2017. The influence of partial isomorphic substitution on electronic and optical parameters of $ABSO_4$-group crystals. Acta Physica Polonica (at press).

Анотація. *У цій роботі вирощено монокристали $K_x(NH_4)_{2-x}SO_4$ (x ≈ 1.75), які належать до родини сульфату калію–амонію, а також вивчено їхню структуру за кімнатної температури. Досліджено спектральні залежності головних показників заломлення та головних оптичних двопроменезаломлень у видимій області. Вздовж напрямку розповсюдження світла паралельно до головної осі x спостерігаємо аномальну дисперсію подвійного променезаломлення. Відповідно до екстраполяції подвійного променезаломлення на основі апроксимації Зельмеєра показників заломлення, симетрія оптичної індикатриси за кімнатної температури повинна підвищитися на довжині світлової хвилі $\lambda_{IP} ≈ 1350±60$ нм. Це відповідає специфічній «ізотропній точці», визначеній умовою $n_x(\lambda_{IP}) = n_y(\lambda_{IP})$. Цю точку досі не було виявлено ні в кристалах K_2SO_4, ні в $(NH_4)_2SO_4$.*